



Control of Both Myeloid Cell Infiltration and Angiogenesis by CCR1 Promotes Liver Cancer Metastasis Development in Mice

Mathieu Paul Rodero, Constance Auvynet, Lucie Poupel, Behazine Combadière, Christophe Combadière

► To cite this version:

Mathieu Paul Rodero, Constance Auvynet, Lucie Poupel, Behazine Combadière, Christophe Combadière. Control of Both Myeloid Cell Infiltration and Angiogenesis by CCR1 Promotes Liver Cancer Metastasis Development in Mice. *Neoplasia*, 2013, 15 (6), pp.641-648. 10.1593/neo.121866 . hal-01586918

HAL Id: hal-01586918

<https://hal.sorbonne-universite.fr/hal-01586918>

Submitted on 13 Sep 2017

HAL is a multi-disciplinary open access archive for the deposit and dissemination of scientific research documents, whether they are published or not. The documents may come from teaching and research institutions in France or abroad, or from public or private research centers.

L'archive ouverte pluridisciplinaire **HAL**, est destinée au dépôt et à la diffusion de documents scientifiques de niveau recherche, publiés ou non, émanant des établissements d'enseignement et de recherche français ou étrangers, des laboratoires publics ou privés.



Distributed under a Creative Commons Attribution 4.0 International License

Control of Both Myeloid Cell Infiltration and Angiogenesis by CCR1 Promotes Liver Cancer Metastasis Development in Mice^{1,2}

**Mathieu Paul Rodero*, Constance Auvynet*,
Lucie Poupel*, Behazine Combadière*,†
and Christophe Combadière*,†**

*Institut National de la Santé et de la Recherche Médicale, (INSERM) UMR-S 945-IUC and Université Pierre et Marie Curie (Paris 6), Laboratory of Immunity and Infection, Institut Universitaire du Cancer, Paris, France; †Assistance Public-Hôpitaux de Paris, Groupe Hospitalier Pitié-Salpêtrière, Service d'Immunologie, Paris, France

Abstract

Expression of the CC chemokine receptor 1 (CCR1) by tumor cells has been associated with protumoral activity; however, its role in nontumoral cells during tumor development remains elusive. Here, we investigated the role of CCR1 deletion on stromal and hematopoietic cells in a liver metastasis tumor model. Metastasis development was strongly impaired in CCR1-deficient mice compared to control mice and was associated with reduced liver monocyte infiltration. To decipher the role of myeloid cells, sublethally irradiated mice were reconstituted with CCR1-deficient bone marrow (BM) and showed better survival rates than the control reconstituted mice. These results point toward the involvement of CCR1 myeloid cell infiltration in the promotion of tumor burden. In addition, survival rates were extended in CCR1-deficient mice receiving either control or CCR1-deficient BM, indicating that host CCR1 expression on nonhematopoietic cells also supports tumor growth. Finally, we found defective tumor-induced neoangiogenesis (*in vitro* and *in vivo*) in CCR1-deficient mice. Overall, our results indicate that CCR1 expression by both hematopoietic and nonhematopoietic cells favors tumor aggressiveness. We propose CCR1 as a potential therapeutic target for liver metastasis therapy.

Neoplasia (2013) 15, 641–648

Introduction

Chemokines are small chemoattractant cytokines that bind to seven-transmembrane domain G protein-coupled receptors. A large number of chemokines are secreted by most, if not all, tumor cells. They are implicated in a wide spectrum of tumor environment-related processes, including tumor spreading [1], tumor survival [2], and angiogenesis [3]; however, the major effect of chemokines is proposed to be on immune cell recruitment [4].

It is now well described that the infiltration of tumors by leukocytes, and more specifically macrophages, could have a protumoral activity [5]. The tumoral environment progressively reprograms infiltrating macrophages, also termed tumor-associated macrophages (TAMs), resulting in a progressive loss of antitumor activity. This is shown by reduced potency of antigen presentation [6], cell cytotoxicity, Th1 cytokine secretion and enhanced tumor survival, and production of proangiogenic, tissue modeling, and anergistic cytokines [7]. High infiltration of tumors by macrophage-like cells in humans and mice is associated with poor survival [5] and high angiogenesis [8] and has been described to favor metastasis formation and dissemination [9].

The CC chemokine receptor 1 (CCR1) is primarily expressed by cells of myeloid lineage, including monocytes, neutrophils, and

Address all correspondence to: Christophe Combadière, PhD, Institut National de la Santé et de la Recherche Médicale (INSERM) UMR-S945, Laboratory of Immunity and Infection, 6th Floor 91, Bld de l'Hôpital, 75013 Paris Cedex 13, France.
E-mail: christophe.combadiere@upmc.fr

¹This work is supported in part by grants from INSERM, the Institut du Cancer (INCA 2005), the Canceropôle-Ile de France, the Agence Nationale de la Recherche “Cardiovasculaire, Obésité et Diabète” (grant AO5088DS), ANR “blanc” (AO5120DD), and European grant “Innochem” (LSHB-CT-2005-518167). M.P.R. was a recipient of a fellowship from Canceropôle-Ile de France and supported by European grant Innochem 518167. C.A. is a recipient of the Neuropôle de Recherche Francilien. C.C. is the recipient of a contract “Interface” from Assistance Publiques-Hôpitaux de Paris.

²This article refers to supplementary materials, which are designated by Table W1 and Figures W1 to W3 and are available online at www.neoplasia.com.

Received 7 November 2012; Revised 20 March 2013; Accepted 24 March 2013

Copyright © 2013 Neoplasia Press, Inc. All rights reserved 1522-8002/13/\$25.00
DOI 10.1593/neo.121866

dendritic cells but also by some T lymphocytes and intimal smooth muscle-like cells. In a mouse colorectal tumor model, tumor cell invasion, metastasis formation, and myeloid progenitor cell recruitment were inhibited in CCR1^{-/-} mice or after administration of CCR1 pharmacological blockade [10,11], suggesting that CCR1-dependent myeloid infiltration has a protumoral effect. In addition, it has been proposed that CCR1 promotes tumor spreading and angiogenesis by controlling metalloproteinase secretion [12]. In this study, we used a model of liver tumor metastasis development and provided, for the first time, evidence of CCR1 expression by non-tumoral cells favoring hepatocellular metastasis development through control of both mononuclear cell infiltration and angiogenesis.

Materials and Methods

Mice

Female C57Bl/6 mice (Charles River, Lyon, France) were maintained under specific pathogen-free conditions on a 12-hour light-dark cycle. CCR1-deficient mice (CCR1^{-/-}) on C57Bl/6 background were provided by Drs Philippe Murphy and Ji Liang Gao (Laboratory of Molecular Immunology, National Institute of Allergy and Infectious Diseases, National Institutes of Health, Bethesda, MD). CCR1^{-/-} mice were back-crossed eight generations with C57Bl/6 green fluorescent protein [(GFP); C57Bl/6-Tg(UBC-GFP)30Scha/J] mice from The Jackson Laboratory (Bar Harbor, ME) to obtain CCR1^{-/-} GFP mice. GFP expression were detected in all tissues examined and used to track leukocytes after transplantation. Mice used for experiments were 8 to 10 weeks old. Animal experiments were approved by the local Institutional Animal Care and Use Committee of Centre d'Exploration Fonctionnelle, Pitié-Salpêtrière.

Cell Lines

The C57BL/6 dimethylbenzanthracene-induced thymoma EL-4 was maintained in RPMI 1640 (Invitrogen Life Technologies, Paisley, Scotland) supplemented with 10% heat-inactivated fetal calf serum (FCS; Seromed, Berlin, Germany), 2 mM L-glutamine, 1000 U/ml penicillin, 1 mg/ml streptomycin, 250 ng/ml amphotericin B (Invitrogen Life Technologies), and 3 µM 22-ME (Sigma-Aldrich, St Louis, MO).

Tumor Models

C57BL/6 control mice or CCR1^{-/-} mice were injected in the tail vein with 5×10^5 EL-4. In another model, mice received subcutaneous (s.c.) injections of 1×10^5 tumor cells in 100 µl of phosphate-buffered saline (PBS) in the right flank. Tumor size was measured three times a week with calipers, and tumor volume was estimated using the following formula: width × length × (width + length)/2. Mice were sacrificed when the tumor volume reached approximately 3 cm³.

Flow Cytometry

At day 12 after EL-4 tail vein injection, harvested livers were cut into small pieces and digested with 400 units of collagenase D (Roche Diagnostics GmbH, Mannheim, Germany) for 30 minutes. Cell suspensions were filtered through a 70-µm cell strainer (BD Biosciences, Bedford, MA) and isolated with density separation medium (Histopaque 1083; Sigma-Aldrich). Leukocytes were collected, washed in PBS, and labeled for flow cytometry using the following monoclonal antibodies:

antibody to CD11b (anti-CD11b PerCP-Cy5), anti-Ly-6G PE, anti-Ly-6C-biotin, anti-CD4 PE, anti-CD3 Alexa Fluor 488, anti-CD8a Alexa Fluor 647, NK1.1 Alexa Fluor 647, anti-CD11c APC, and streptavidin-PerCP (all sourced from BD Pharmingen, San Diego, CA). Anti-mouse neutrophil 7/4 Alexa Fluor 488 and Alexa Fluor 647 were from AB Serotec (Oxford, United Kingdom). Cell suspensions were incubated with appropriate fluorochrome-conjugated monoclonal antibodies and analyzed on a FACSCalibur cytofluorimeter (Becton Dickinson, Franklin Lakes, NJ). Results were analyzed with CellQuest Pro software (Becton Dickinson).

Bone Marrow Chimeras

Control and CCR1^{-/-} recipient mice were irradiated with 10-Gy radiation using an ORION linear accelerator (General Electric Healthcare, Milwaukee, WI). Whole bone marrow (BM) from either control GFP mice [C57BL/6-Tg(UBC-GFP)30Scha/J] or transgenic CCR1^{-/-} GFP (see Mice section) was extracted from the tibia and femur. Donor cells (5×10^6) were injected into recipient mice through the retro-orbital vein. Twelve weeks after transplant, recipient mice were injected with EL-4 thymoma cells.

Aortic Rings

Control and CCR1^{-/-} mice aortas were isolated and cut into small segments. These were placed in Matrigel (BD Biosciences)-coated 42-well plates containing 10% FCS in Dulbecco's modified Eagle's medium (DMEM) culture medium. Cultures were incubated at 37°C and 5% CO₂ for 6 days, and explants were monitored for sprouting vessels. For the EL-4-conditioned medium experiments, cultured media were removed from wells after 3 days and replaced by 50% DMEM, 10% FCS + 50% RPMI, 10% FCS or 50% DMEM, 10% FCS + 50% EL-4-conditioned RPMI, 10% FCS. After fixation and 4',6-diamidino-2-phenylindole (DAPI; Sigma-Aldrich) staining, vessel formation was quantified by measuring the area of vessel-like extensions from the explants using ImageJ 1.39U software.

CD31 and Lectin Immunohistochemical Staining

At day 12 after EL-4 tail vein injection, 6-µm frozen liver sections from control and CCR1^{-/-} mice were fixed with 4% paraformaldehyde for 10 minutes, washed three times for 5 minutes in PBS, and incubated overnight at 4°C with anti-CD31 (AB Serotec) or anti-lectin (Sigma-Aldrich) antibody. CD31 staining was visualized with r-phycocerythrin (RPE)-conjugated anti-rabbit Ig antibody (Invitrogen, Carlsbad, CA). Lectin- and CD31-positive areas in tumoral and non-tumoral livers were visualized by scanning sections at low magnification (×20). The number of microvessels was recorded in six randomly chosen fields of view using ImageJ 1.39U software.

Reverse Transcription–Polymerase Chain Reaction

Total RNA was extracted from sorted hepatic endothelial cells (ECs), peripheral blood mononuclear cells (PBMCs), or cultured EL-4 using Qiagen Micro Kit (Qiagen, Hilden, Germany), according to the manufacturer's instructions. Total RNA was reverse transcribed to cDNA using SupertScript Reverse Transcriptase (Invitrogen). Real-time polymerase chain reaction was carried out using SYBR Premix (Invitrogen) with the primer sets described in Table W1. To standardize mRNA concentrations, transcript levels of *glyceraldehyde 3-phosphate dehydrogenase* (GAPDH) were determined in parallel for each sample, and relative transcript levels were corrected by normalization on the basis of GAPDH transcript levels.

Statistical Analysis

Mann-Whitney test and/or log-rank (Mantel-Cox) test were used to determine whether variation in experimental groups was significant using GraphPad Prism software (GraphPad, San Diego, CA).

Results

CCR1 Deficiency Increases Survival in Tumor Metastasis Engraftment Models

After IV injection of control C57BL/6 mice into the tail vein, EL-4 thymoma cells selectively grew in the liver and kidney. The mortality occurred approximately 3 weeks after tumor cell injection, and after 32 days, all of the mice had died (Figure 1A). Interestingly, in this tumor model, the CCR1-deficient mice (CCR1^{-/-}) survived longer than control mice, with a mean survival of 27.5 and 23 days, respectively (Figure 1A). In addition, 20 days after IV tumor cell injection, livers from CCR1^{-/-} mice were much smaller in size than those from control mice, 2.1 ± 0.2 and 3.4 ± 0.4 g, respectively (Figure 1B). To confirm the role of CCR1 in tumor growth, we set up a second model in which tumor cells were injected s.c. While all control mice developed palpable tumors 6 days after s.c. injection, only half of the CCR1^{-/-} mice showed the presence of tumors at day 8 (Figure 1C). After 3 weeks, 30% of the CCR1^{-/-} mice remained tumor-free, as opposed to all of the control mice that had developed tumors. The

mean volume of EL-4 tumors in CCR1^{-/-} mice was less than in control mice at all time points (Figure 1D). These results indicate that host cell CCR1 expression favors tumor aggressiveness.

CCR1 Deficiency Is Associated with Decreased Infiltration of Myeloid Cells into Tumors

To better understand how CCR1 activation may promote liver metastasis development, we analyzed the leukocyte infiltration during early stages of tumor development. Analyses were performed 12 days after IV tumor injection in the liver and the kidney. At this stage, tumor foci are undetectable macroscopically. Using flow cytometry, we identified tumor cell infiltrates as myeloid infiltrates based on CD11bhi and NK 1.1neg expression (gate 1 in Figure 2A, left panel). Inflammatory monocytes were discriminated from the so-called “patrolling” monocytes based on 7/4 expression level [13] (gates 2 and 3 in Figure 2A, right panel). There was a strict co-expression between 7/4 marker and Ly6C, the marker commonly used to discriminate monocyte subpopulations as previously published [13] (in Supplementary data). Inflammatory monocytes were defined as 7/4hi, Ly6Chi, Ly6Gneg cells and resident monocytes as 7/4lo, Ly6Cint/lo, Ly6Gneg cells. Neutrophils were defined as 7/4hi Ly6Chi Ly6Ghi cells (gate 4). CD4 and CD8 lymphocytes were defined as, respectively, CD3+ CD4+ NK1.1- and CD3+ CD8+ cells, whereas NK cells were defined as CD3- NK1.1+ cells and NKT as CD3+ NK1.1+ cells (not

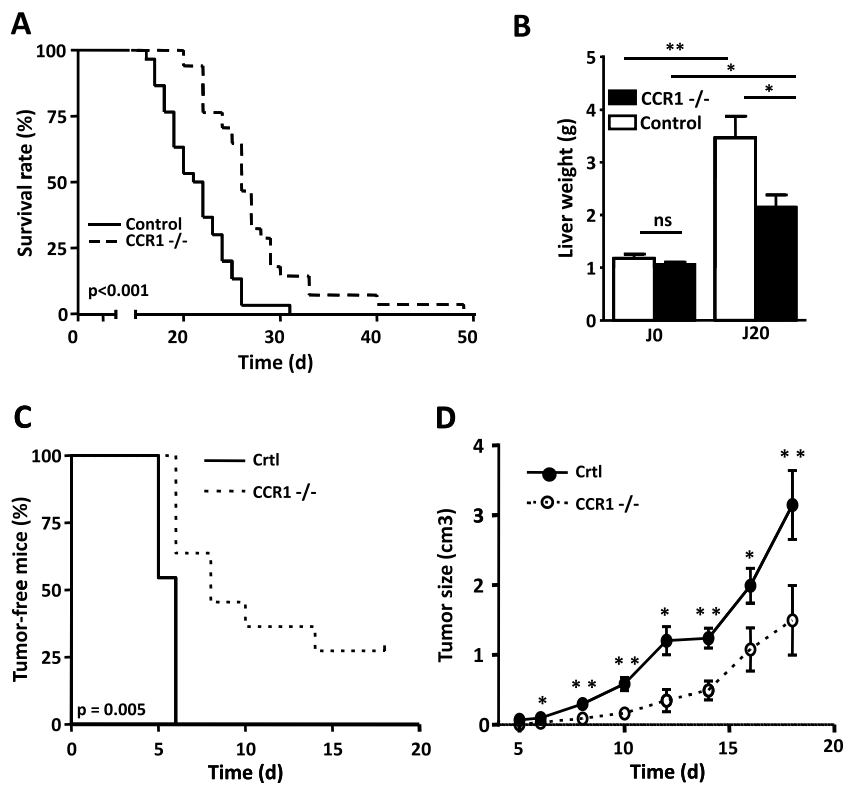


Figure 1. Lack of CCR1 reduces tumor development. (A) Survival curve of C57BL/6 control mice (solid line) or C57BL/6 CCR1^{-/-} mice (dotted line) injected IV with 5×10^5 EL-4. Mean survival time of CCR1^{-/-} mice ($n = 28$) was 20% longer than in control mice ($n = 19$). (B) Twenty-one days after tumor inoculation, the increase in liver weight is smaller in CCR1^{-/-} mice compared to WT mice. Each data point represents the mean tumoral liver weight \pm SEM of 10 mice. (C) CCR1^{-/-} mice ($n = 11$) showed delay tumor appearance compared to control mice (solid line, $n = 11$), log-rank test, $P = .005$. (D) Tumor size growth in control mice (solid line, $n = 11$) or CCR1^{-/-} mice ($n = 11$) injected s.c. with 1×10^5 EL-4. Tumor development is delayed in CCR1^{-/-} mice. * $P < .05$; ** $P < .01$ (mice with tumor size of $>3 \text{ cm}^3$ were killed).

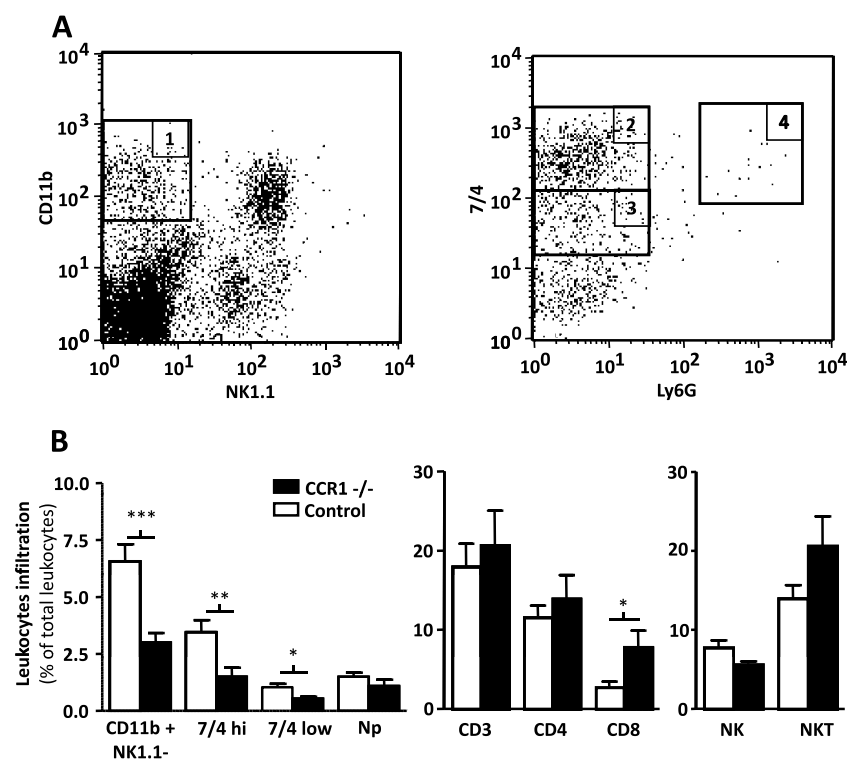


Figure 2. CCR1 deficiency alters leukocyte recruitment at the tumor site. (A) Dot plot analysis identified tumoral leukocyte subpopulation infiltrates by flow cytometry analysis: 1, myeloid cells; 2, inflammatory monocytes; 3, resident monocytes; 4, neutrophils. (B) CCR1^{-/-} mice show defect in the myeloid cell mobilization, mainly due to a defect recruitment of the 7/4⁺ monocyte population. Percentages \pm SEM were indicated for each group (control in black, $n = 10$; CCR1^{-/-} in white, $n = 10$) and were obtained from two independent experiments. Np, neutrophils; significant value of $*P < .05$, $**P < .001$, and $***P < .0001$.

shown). Interestingly, a major effect on leukocyte recruitment in the CD11b⁺ myeloid compartment was observed (Figure 2B, left panel), with a 50% reduction in CCR1^{-/-} mouse liver (6.6% and 3% of total cells, respectively, $P < .001$). This was associated with reduced infiltration of both inflammatory (3.5% and 1.5%, $P = .005$) and “patrolling” monocytes (1% and 0.5%, $P = .014$). We did not observe any significant differences in the neutrophil infiltrate. In the lymphocyte compartment (Figure 2B, middle panel), only CD3⁺ CD8⁺ cells were

present in larger number in the livers of CCR1^{-/-} mice compared to those of control mice (Figure 3B; $P = .043$), whereas CD3⁺ CD4⁺, NK, and NKT cells were unaltered (Figure 3B, middle and right panels). Analysis of the kidney infiltrates showed similar trends with reduced monocyte and CD8⁺ cell infiltration (Figure W1). The concomitant decrease of TAM infiltration, with the increase of cytotoxic CD8 T cells, may indicate a better control of tumor immunosuppression by the immune system in CCR1^{-/-} mice.

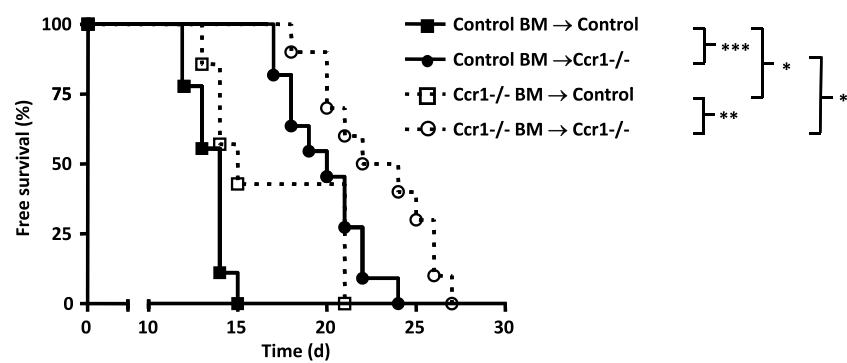


Figure 3. CCR1 expression by both BM and non-BM-derived cells promotes tumor metastasis. Survival curve of CCR1^{-/-} and control chimeric mice injected IV with 5×10^5 EL-4. Chimeric mice resulted from control and CCR1^{-/-} irradiated hosts reconstituted with CCR1^{-/-} GFP or control GFP BM. CCR1^{-/-} hosts with control BM (open squares; $n = 7$) and WT host with control BM (filled squares; $n = 9$) had significantly decreased mean survival than mice of the same genotype with CCR1 BM, respectively, WT host with CCR1 BM (open circles; $n = 10$) and CCR1 host with CCR1 BM (filled circles; $n = 11$ mice).

Protumoral Effect of CCR1 Is Due to Expression on Both Hematopoietic and Nonhematopoietic Cells

We hypothesized that in addition to CCR1-driven protumoral leukocyte recruitment, nonhematopoietic cells expressing CCR1 may also favor tumor growth, as proposed previously for CCR5 [14]. To delineate the contribution of CCR1 on hematopoietic cells compared to nonhematopoietic cells, we performed BM chimera experiments. We first assessed the effect of CCR1 deletion on leukocyte subpopulation engraftment. The distributions of lymphocytes, NK, monocytes, and neutrophils in the blood of wild type (WT) mice irradiated and reconstituted with WT or CCR1^{-/-} BM or in the blood of CCR1^{-/-} mice irradiated and reconstituted with WT BM were unchanged, indicating that the lack of CCR1 expression by either hematopoietic or nonhematopoietic cells did not alter engraftment (Figure W2). CCR1^{-/-} and control mice were sublethally irradiated and reconstituted with BM cells from either GFP control or CCR1^{-/-} GFP transgenic mice (Figure 3). All mice showed greater than 90% of GFP-positive leukocytes (data not shown). After EL-4 IV injection, both control (open squares) and CCR1^{-/-} recipient (open circles) mice showed increased survival when reconstituted with CCR1^{-/-} BM compared to their respective controls, with median survival of 14 and 20 days ($P < .001$) and 15 and 23 days ($P = .01$), respectively. This indicates that hematopoietic cell CCR1 expression favors EL-4 burden. Surprisingly, survival rates were extended in CCR1^{-/-} mice receiving either control (filled circles) or CCR1^{-/-} (open circle) BM, with median survival of 20 and 23 days ($P = .018$). This suggests that the expression of CCR1 by nonhematopoietic cells also contributes to tumor growth.

Lack of CCR1 Led to Reduce Hepatic Capillary Density during Early-Stage Tumor Development

We postulated that CCR1 may also control metastasis development by regulating tumor-induced vascularization. To test this hypothesis, we measured the blood capillary density in the control or CCR1^{-/-} mouse livers at a time point where tumors were not macroscopically detectable (Figure 4A, left and right panels, respectively). Twelve days

after tumor inoculation, the liver microvessel density as assessed by CD31 staining was increased by more than three-fold ($P = .004$) in control mice, whereas it was only modestly increased in CCR1^{-/-} mice (Figure 4B). Similar results were obtained with lectin staining (Figure W3). These results indicated that tumor development is associated with enhanced hepatic capillary density before we could detect the tumoral foci and strongly suggested that CCR1 promoted tumor-associated vascularization of the liver.

CCR1 Deficiency Led to Reduced Monocyte-Independent Neoangiogenesis

Because CCR1 may favor tumor-associated vascularization, we investigated the role of CCR1 in an *in vitro* angiogenesis model supposedly independent of the circulating leukocytes. We compared the vessel sprouting around aortic ring from control and CCR1^{-/-} mice (Figure 5A, left and right panels, respectively). After 6 days in culture, the area of vessel-like extensions from CCR1^{-/-} explants was about 50% smaller than those of control explants (Figure 5B). These data suggest that CCR1 promotes EC outgrowth, independent of recruited myeloid cell with proangiogenic properties. To further investigate the mechanism associated with EL-4-induced angiogenesis in the liver, we compared the vessel sprouting around aortic ring from control and CCR1^{-/-} mice in the presence of EL-4-conditioned media. EL-4 supernatant increased vessel sprouting from WT mouse aortic ring compared to control media by 55% ($P = .0085$). In these conditions, vessel sprouting of CCR1^{-/-} aortic ring was strongly inhibited (57%, $P < .001$), indicating that EL-4 promoted CCR1-dependent angiogenesis in a hematopoietic-independent model. To support the hypothesis that similar mechanisms may take place in the tumor microenvironment, we investigated the expression of *CCR1* in sorted hepatic ECs (Figure 5C) and of its ligands in the EL-4 tumoral cell line (Figure 5D). *CCR1* transcripts were strongly expressed in PBMCs and were also detected in hepatic ECs. EL-4 expressed high level of *CCL5* but no *CCL3*, indicating that EL-4 secretion may directly

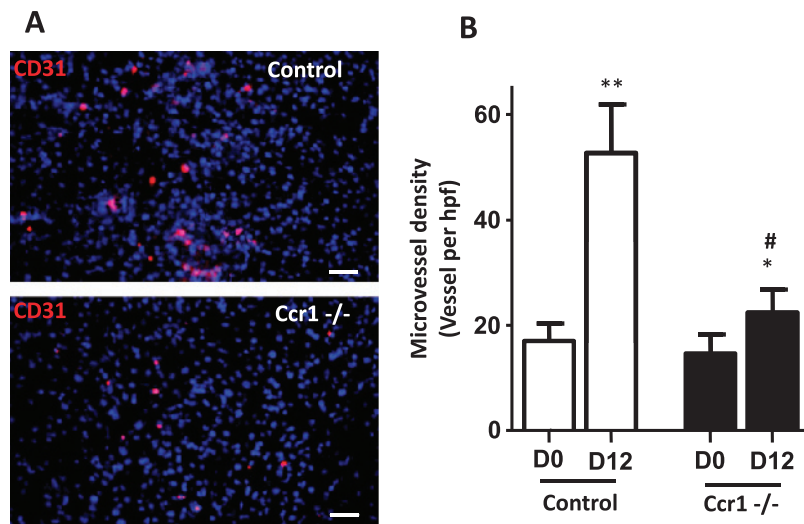


Figure 4. Reduced numbers of microvessels in tumoral liver of CCR1^{-/-} mice. (A) Frozen liver sections from CCR1^{-/-} and control mice injected with tumor cells were stained with anti-CD31 antibody. Control staining was performed by only incubating with the secondary antibody. (B) Number of microvessels were counted in six randomly chosen fields. Each value represents mean \pm SEM ($n = 6$). * $P < .05$, ** $P < .001$ compared to D0, # $P < .05$ compared to control mice.

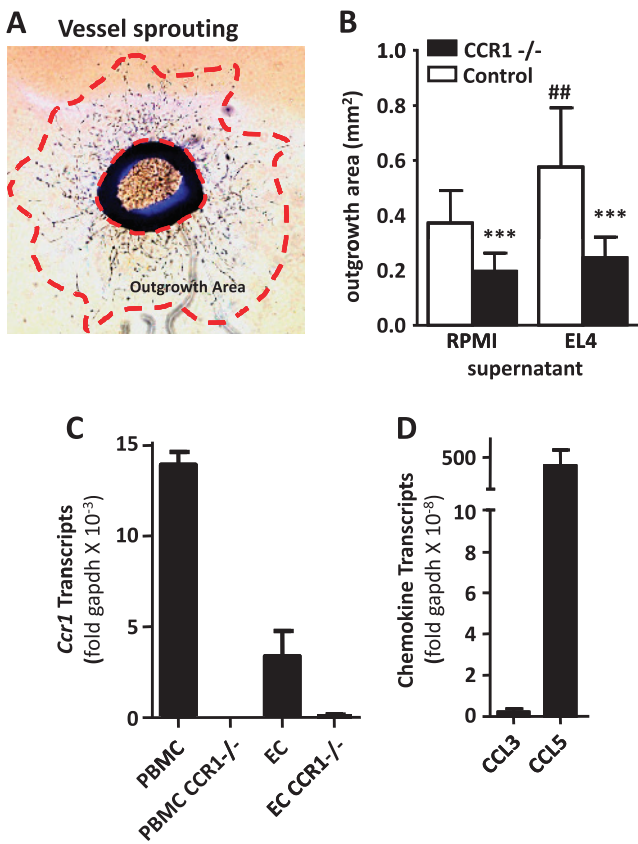


Figure 5. Lack of CCR1 reduces neoangiogenesis in a vessel sprouting assay. (A) Representative photomicrograph of aortic ring with vessel sprouting. The outgrowth area was measured between the vessel growth front and the base of the aortic ring. (B) Vessel sprouting in control and CCR1-deficient aortic ring. Outgrowth area was measured in the absence or presence of EL-4-conditioned media. Each value represents mean area \pm SEM ($n = 12$). (C) Level of *Ccr1* transcripts in hepatic ECs and PBMCs from WT and CCR1 $^{-/-}$ mice. ECs were isolated by flow cytometry and defined as CD45–F4/80–CD31+ cells. (D) Level of CCR1 ligand transcripts (CCL3 and CCL5) in EL-4. *** $P < .001$ compared to WT and ## $P < .01$ compared to control media.

activate hepatic ECs. Altogether, these data support the model of CCR1-triggered angiogenesis in the absence of hematopoietic cells.

Discussion

While lymphocyte infiltration is usually associated with good prognosis [15], tumor-associated myeloid lineage cells are almost always associated with poor survival, increased tumor spreading, and metastases [5]. The roles of several chemokines in controlling human tumor development or spreading have been well demonstrated [16]. Several polymorphisms in human chemokine genes affect patient prognosis markers, possibly by controlling TAM recruitment [17,18]. The protumoral effect of CCR1 by tumor cells has been described in several mouse tumor models [19–22]. This study focused on the role of CCR1, expressed by stromal cells but not tumor cells. Our data indicate that tumor development is impaired in CCR1 $^{-/-}$ mice, in both the tumor metastasis implantation model and tumor growth model, compared to control mice. We showed that CCR1 expression on both hematopoietic and nonhematopoietic cells impaired mouse survival.

The better survival of the CCR1 $^{-/-}$ mice is associated with both the reduction in infiltration of myeloid lineage cells and highest level of infiltration of CD8 T cells. Moreover, angiogenesis is defective in CCR1 $^{-/-}$ mice both *in vivo* and *in vitro*.

It was previously proposed that CCR1 controls immature myeloid cell recruitment in tumors, therefore promoting tumor development [10,11]. Here, we show that CCR1 is also involved in the recruitment of mature myeloid cells, mainly altering monocyte but not neutrophil infiltration. Although neutrophils express CCR1, the kinetics of their recruitment may differ from that of monocytes. Alternatively, neutrophils may be recruited by other tumor-secreted chemokines, such as Cxcl8, which could compensate for the lack of CCR1. CCR1 deficiency affects slightly more inflammatory monocyte infiltration than “patrolling” monocyte infiltration. Some chemokine receptors, like Ccr2 or Cx3cr1, are known to be differentially expressed by these subsets of monocytes, but there are no clear evidences concerning CCR1 [23]. However, a previous report indicated that the CCR1 RNA expression level is two to three times higher in 7/4hi monocytes than 7/4lo from the blood [24]. Nonetheless, the implication of CCR1 in migratory properties of different subsets of monocytes should be completed to confirm that CCR1 is preferentially implicated in 7/4hi monocyte migration than 7/4lo monocyte migration. We also observed enhanced CD8 T lymphocyte infiltration in CCR1 $^{-/-}$ mice, likely to result from the tumor microenvironment alteration in CCR1 $^{-/-}$ mice. Globally, both reduction in the protumoral myeloid compartment and enhanced cytotoxic CD8 T cell infiltration may play a role in the improved control of tumor development in CCR1 mice. The role of CCR1 expressed by nontumoral cells remains ambiguous in tumor development. Although the expression of CCR1 by cells of myeloid lineage may promote tumor development, several models support the idea that CCR1 may favor antitumor immune response when tumor immunotolerance is thwarted. For instance, the antitumoral effect of radiofrequency ablation was enhanced by an agonist of CCR1 in a murine hepatocellular carcinoma model. This effect was associated with increased infiltration of the radiofrequency ablation-treated tumor by lymphocytes and CCR1-positive dendritic cells. In CCR1 $^{-/-}$ mice, both the leukocyte recruitment and antitumor effect, induced by the CCR1 agonist, were inhibited [25]. Taken together, the CCR1 axis may control the subtle balance between innate protumoral activity and adaptative antitumoral responses.

The tumor-induced vascular capillary density was reduced in CCR1-deficient mice. These results confirm previous observation made by Yang et al. in a model of induced hepatocellular carcinoma [12], although our data indicated that this effect was dependent on host CCR1 expression and not due to tumor cells that were CCR1 competent. The cellular origin of the neovasculature in this model is not clearly established, as the ability of BM-derived cells to integrate vessel has been proposed in an aggressive tumor model. However, we demonstrated that EL-4 supernatant promotes angiogenesis *ex vivo* independently of hematopoietic cells. Moreover, the vessel density was measured before macroscopic tumor detection, suggesting that, at that time, mostly hepatic vasculature was altered. Hence, even if we cannot exclude it, the contribution of hematopoietic cells in the formation of the neovessel wall is likely to be minor. Consistent with previous studies performed with CCR5 $^{-/-}$ mice [14], we demonstrated, using BM transfer experiments, that tumor aggressiveness is not only dependent on CCR1 expression by stromal hematopoietic cells but also on its expression by stromal nonhematopoietic cells. Indeed, stromal nonhematopoietic cells have already been associated

with tumor development, promoting angiogenesis [26] or metastasis formation [27]. Surprisingly, when irradiated and reconstituted with BM from control mice, CCR1-deficient mice have a longer survival than irradiated control mice reconstituted with homologous control BM. This indicates that CCR1 expression by nonhematopoietic cells also contributes to tumor aggressiveness. The angiogenesis aortic ring model, with or without condition media from EL-4 culture, confirmed that EL-4 secreted cytokines that promote angiogenesis in the absence of hematopoietic cells by CCR1-dependent mechanism. It is not clear which cell population, present in the aorta, controls new capillary formation in a CCR1-dependent mechanism. However, we showed here that CCR1 mRNA was expressed by hepatic EC. These results are in accordance with previous work showing the expression of CCR1 mRNA by rat EC [28] and the ability of human EC lines to migrate and differentiate when stimulated with a CCR1 agonist [29]. Moreover, the high expression of CCL5 transcript, but not CCL3, by EL-4 was consistent with the direct proangiogenic effect of CCL5 through binding on CCR1 expressed by EC [30]. In addition, the mesenchymal stem cells present in the media of the aorta express CCR1 transcript [31], and recent insights support the role of CCR1 expression by mesenchymal stem cells in angiogenesis [32]. We show that the protumoral effect of CCR1 was mediated by both hematopoietic and nonhematopoietic CCR1-expressing cells. However, the relative importance of each compartment remains unclear. The percentage of recruitment of only some leukocyte populations is affected in CCR1 null mice, suggesting that these defects of recruitment did not result from reduced angiogenesis. In addition, the concomitant defect in infiltration of the tumor by monocytes and strong diminution of the capillary density in CCR1^{-/-} is consistent with our recent finding that inflammatory monocytes promote post-ischemic neovascularization [33]. Interestingly, we did not observe any differences when we compared the hepatic artery network by microangiography in control and CCR1^{-/-} mice, 12 days after EL-4 injection (data not shown). These data suggest that the role of CCR1 on angiogenesis is restricted to capillary vessels, and not larger arteries, at least during early-stage metastasis development.

In conclusion, we showed that both hematopoietic and stromal cells participate in CCR1-dependent protumoral activity. CCR1 deficiency limited tumor progression and increased mouse survival rates. These beneficial effects were associated with reduced monocyte mobilization and reduced tumoral neovascularization. Further experiments should be performed to confirm the pertinence of using CCR1 as a therapeutic target in the control of metastasis development.

Acknowledgments

The authors thank Cangialosi Arnaud, Godart Jeremy, and Potier Yann for technical mouse assistance. The authors also thank Vilar José for technical assistance, Catherine Blanc for her help in cell sorting, and Rebecca Ellis for her assistance in preparing the manuscript.

References

- [1] Muller A, Homey B, Soto H, Ge N, Catron D, Buchanan ME, McClanahan T, Murphy E, Yuan W, Wagner SN, et al. (2001). Involvement of chemokine receptors in breast cancer metastasis. *Nature* **410**, 50–56.
- [2] Barbero S, Bonavia R, Bajetto A, Porcile C, Pirani P, Ravetti JL, Zona GL, Spaziante R, Florio T, and Schettini G (2003). Stromal cell-derived factor 1 α stimulates human glioblastoma cell growth through the activation of both extracellular signal-regulated kinases 1/2 and Akt. *Cancer Res* **63**, 1969–1974.
- [3] Strieter RM, Kunkel SL, Elner VM, Martonyi CL, Koch AE, Polverini PJ, and Elner SG (1992). Interleukin-8. A corneal factor that induces neovascularization. *Am J Pathol* **141**, 1279–1284.
- [4] Balkwill F and Mantovani A (2001). Inflammation and cancer: back to Virchow? *Lancet* **357**, 539–545.
- [5] Lewis CE and Pollard JW (2006). Distinct role of macrophages in different tumor microenvironments. *Cancer Res* **66**, 605–612.
- [6] Loercher AE, Nash MA, Kavanagh JJ, Platsoucas CD, and Freedman RS (1999). Identification of an IL-10-producing HLA-DR-negative monocyte subset in the malignant ascites of patients with ovarian carcinoma that inhibits cytokine protein expression and proliferation of autologous T cells. *J Immunol* **163**, 6251–6260.
- [7] Mantovani A, Allavena P, and Sica A (2004). Tumour-associated macrophages as a prototypic type II polarised phagocyte population: role in tumour progression. *Eur J Cancer* **40**, 1660–1667.
- [8] Leek RD and Harris AL (2002). Tumor-associated macrophages in breast cancer. *J Mammary Gland Biol Neoplasia* **7**, 177–189.
- [9] Lin EY, Nguyen AV, Russell RG, and Pollard JW (2001). Colony-stimulating factor 1 promotes progression of mammary tumors to malignancy. *J Exp Med* **193**, 727–740.
- [10] Kitamura T, Kometani K, Hashida H, Matsunaga A, Miyoshi H, Hosogi H, Aoki M, Oshima M, Hattori M, Takabayashi A, et al. (2007). SMAD4-deficient intestinal tumors recruit CCR1⁺ myeloid cells that promote invasion. *Nat Genet* **39**, 467–475.
- [11] Kitamura T, Fujishita T, Loetscher P, Revesz L, Hashida H, Kizaka-Kondoh S, Aoki M, and Taketo MM (2010). Inactivation of chemokine (C-C motif) receptor 1 (CCR1) suppresses colon cancer liver metastasis by blocking accumulation of immature myeloid cells in a mouse model. *Proc Natl Acad Sci USA* **107**, 13063–13068.
- [12] Yang X, Lu P, Fujii C, Nakamoto Y, Gao JL, Kaneko S, Murphy PM, and Mukaida N (2006). Essential contribution of a chemokine, CCL3, and its receptor, CCR1, to hepatocellular carcinoma progression. *Int J Cancer* **118**, 1869–1876.
- [13] Combadiere C, Potteaux S, Rodero M, Simon T, Pezard A, Esposito B, Merval R, Proudfoot A, Tedgui A, and Mallat Z (2008). Combined inhibition of CCL2, CX3CR1, and CCR5 abrogates Ly6C^{hi} and Ly6C^{lo} moncytosis and almost abolishes atherosclerosis in hypercholesterolemic mice. *Circulation* **117**, 1649–1657.
- [14] van Deventer HW, O'Connor W Jr, Brickey WJ, Aris RM, Ting JP, and Serody JS (2005). C-C chemokine receptor 5 on stromal cells promotes pulmonary metastasis. *Cancer Res* **65**, 3374–3379.
- [15] Bordignon C, Carlo-Stella C, Colombo MP, De Vincentiis A, Lanata L, Lemoli RM, Locatelli F, Olivieri A, Rondelli D, Zanon P, et al. (1999). Cell therapy: achievements and perspectives. *Haematologica* **84**, 1110–1149.
- [16] Lazennec G and Richmond A (2010). Chemokines and chemokine receptors: new insights into cancer-related inflammation. *Trends Mol Med* **16**, 133–144.
- [17] Rodero M, Marie Y, Coudert M, Blondet E, Mokhtari K, Rousseau A, Raoul W, Carpenter C, Sennlaub F, Deterre P, et al. (2008). Polymorphism in the microglial cell-mobilizing CX3CR1 gene is associated with survival in patients with glioblastoma. *J Clin Oncol* **26**, 5957–5964.
- [18] Rodero M, Rodero P, Descamps V, Lebbe C, Wolkenstein P, Aegeyer P, Vitoux D, Basset-Seguin N, Dupin N, Grandchamp B, et al. (2007). Melanoma susceptibility and progression: association study between polymorphisms of the chemokine (CCL2) and chemokine receptors (CX3CR1, CCR5). *J Dermatol Sci* **46**, 72–76.
- [19] Wang CL, Sun BS, Tang Y, Zhuang HQ, and Cao WZ (2009). CCR1 knockdown suppresses human non-small cell lung cancer cell invasion. *J Cancer Res Clin Oncol* **135**, 695–701.
- [20] Wu X, Fan J, Wang X, Zhou J, Qiu S, Yu Y, Liu Y, and Tang Z (2007). Downregulation of CCR1 inhibits human hepatocellular carcinoma cell invasion. *Biochem Biophys Res Commun* **355**, 866–871.
- [21] Menu E, De Leenheer E, De Raeve H, Coulton L, Imanishi T, Miyashita K, Van Valckenborgh E, Van Riet I, Van Camp B, Horuk R, et al. (2006). Role of CCR1 and CCR5 in homing and growth of multiple myeloma and in the development of osteolytic lesions: a study in the 5TMM model. *Clin Exp Metastasis* **23**, 291–300.
- [22] Lu P, Nakamoto Y, Nemoto-Sasaki Y, Fujii C, Wang H, Hashii M, Ohmoto Y, Kaneko S, Kobayashi K, and Mukaida N (2003). Potential interaction between CCR1 and its ligand, CCL3, induced by endogenously produced interleukin-1 in human hepatomas. *Am J Pathol* **162**, 1249–1258.
- [23] Geissmann F, Jung S, and Littman DR (2003). Blood monocytes consist of two principal subsets with distinct migratory properties. *Immunity* **19**, 71–82.

- [24] Tacke F, Alvarez D, Kaplan TJ, Jakubzick C, Spanbroek R, Llodra J, Garin A, Liu J, Mack M, van Rooijen N, et al. (2007). Monocyte subsets differentially employ CCR2, CCR5, and CX3CR1 to accumulate within atherosclerotic plaques. *J Clin Invest* **117**, 185–194.
- [25] Iida N, Nakamoto Y, Baba T, Nakagawa H, Mizukoshi E, Naito M, Mukaida N, and Kaneko S (2010). Antitumor effect after radiofrequency ablation of murine hepatoma is augmented by an active variant of CC chemokine ligand 3/macrophage inflammatory protein-1 α . *Cancer Res* **70**, 6556–6565.
- [26] Orimo A, Gupta PB, Sgroi DC, Arenzana-Seisdedos F, Delaunay T, Naeem R, Carey VJ, Richardson AL, and Weinberg RA (2005). Stromal fibroblasts present in invasive human breast carcinomas promote tumor growth and angiogenesis through elevated SDF-1/CXCL12 secretion. *Cell* **121**, 335–348.
- [27] Vizoso FJ, Gonzalez LO, Corte MD, Rodriguez JC, Vazquez J, Lamelas ML, Junquera S, Merino AM, and Garcia-Muniz JL (2007). Study of matrix metalloproteinases and their inhibitors in breast cancer. *Br J Cancer* **96**, 903–911.
- [28] Thomas RA, Pietrzak DC, Scicchitano MS, Thomas HC, McFarland DC, and Frazier KS (2009). Detection and characterization of circulating endothelial progenitor cells in normal rat blood. *J Pharmacol Toxicol Methods* **60**, 263–274.
- [29] Hwang J, Son KN, Kim CW, Ko J, Na DS, Kwon BS, Gho YS, and Kim J (2005). Human CC chemokine CCL23, a ligand for CCR1, induces endothelial cell migration and promotes angiogenesis. *Cytokine* **30**, 254–263.
- [30] Suffee N, Hlawaty H, Meddahi-Pelle A, Maillard L, Louedec L, Haddad O, Martin L, Laguillier C, Richard B, Oudar O, et al. (2012). RANTES/CCL5-induced pro-angiogenic effects depend on CCR1, CCR5 and glycosaminoglycans. *Angiogenesis* **15**, 727–744.
- [31] Brooke G, Tong H, Levesque JP, and Atkinson K (2008). Molecular trafficking mechanisms of multipotent mesenchymal stem cells derived from human bone marrow and placenta. *Stem Cells Dev* **17**, 929–940.
- [32] Huang J, Zhang Z, Guo J, Ni A, Deb A, Zhang L, Mirotsov M, Pratt RE, and Dzau VJ (2010). Genetic modification of mesenchymal stem cells overexpressing CCR1 increases cell viability, migration, engraftment, and capillary density in the injured myocardium. *Circ Res* **106**, 1753–1762.
- [33] Cochain C, Rodero MP, Vilar J, Recalde A, Richart A, Loinard C, Zouggari Y, Guerin C, Duriez M, Combadiere B, et al. (2010). Regulation of monocyte subsets systemic levels by distinct chemokine receptors controls postischemic neovascularization. *Cardiovasc Res* **88**, 186–195.

Table W1. RT-PCR Primer Sequences.

| Genes | Forward | Reverse |
|--------------|--------------------------|-------------------------|
| <i>CCL5</i> | GCTGCCCTCACCATCATCCTCACT | GGCACACACTGGCGGTTCTTC |
| <i>CCL3</i> | GTGCCCTTGCCTGTTGTGTGAT | CTGCCGGTTCTCTCGTCAGGA |
| <i>CCR1</i> | TTAGCTTCCATGCCTGCCTTATA | TCCACCTGCTTCAGGCTCTTGT |
| <i>GAPDH</i> | CCTGGAGAACCTGCCAAGTATG | AGAGTGGGAGTTGCTGTTGACTC |

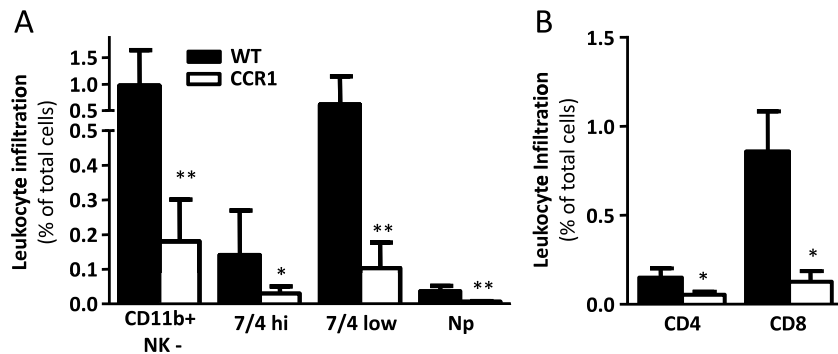


Figure W1. CCR1 deficiency alters leukocyte recruitment at the tumor site. (A) CCR1^{-/-} mice showed defects in the myeloid and lymphoid cell mobilization in the kidney at day 12 post-tumor inoculation. Percentages (\pm SEM) were indicated for each group (control in black, $n = 5$; CCR1^{-/-} in white, $n = 5$). Np, neutrophils; significant value of $*P < .05$ and $**P < .001$.

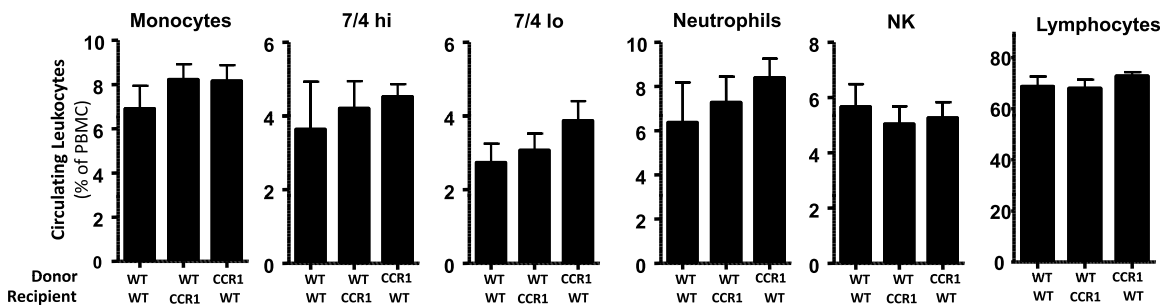


Figure W2. CCR1 expression by hematopoietic or nonhematopoietic cells do not alter the peripheral leukocyte distribution after BM transfer. Percentages of circulating total monocytes, inflammatory monocytes, resident monocytes, neutrophils, NK, and lymphocytes were evaluated 8 weeks after irradiation of WT or CCR1^{-/-} recipients reconstituted with WT or CCR1^{-/-} BM; $n = 3$ to 5 mice.

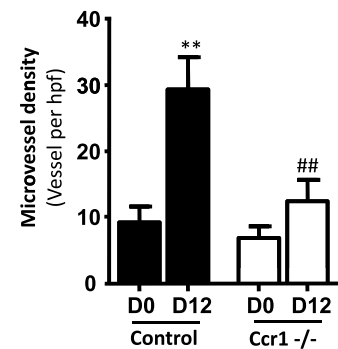


Figure W3. Reduced numbers of microvessels in tumoral liver of CCR1^{-/-} mice. Frozen liver sections from CCR1^{-/-} and control mice injected with tumor cells were stained with lectin antibody. The number of microvessels was counted in six randomly chosen fields. Each value represents mean \pm SEM ($n = 6$ to 8). ** $P < .01$ compared to D0; ## $P < .01$ compared to control mice.